1-1-2019

Evidence for the Early Evolutionary Loss of the M20D Auxin Amidohydrolase Family from Mosses and Horizontal Gene Transfer from Soil Bacteria of Cryptic Hydrolase Orthologues to Physcomitrella patens

James Campanella
Montclair State University, campanellj@mail.montclair.edu

Stephanie Kurdach
Bergen Community College

Richard Skibitski
Technische Universität Dresden

John V. Smalley
Bergen Community College

Samuel Desind
Montclair State University

Journal of Plant Growth Regulation (2019) 38:1428–1438
https://doi.org/10.1007/s00344-019-09945-6

Evidence for the Early Evolutionary Loss of the M20D Auxin Amidohydrolase Family from Mosses and Horizontal Gene Transfer from Soil Bacteria of Cryptic Hydrolase Orthologues to *Physcomitrella patens*

James J. Campanella[1] · Stephanie Kurdach[1] · Richard Skibitski[1] · John V. Smalley[1,2] · Samuel Desind[1] · Jutta Ludwig-Müller[3]

Received: 20 September 2018 / Accepted: 29 January 2019 / Published online: 16 March 2019

Abstract

Inactive auxin conjugates are accumulated in plants and hydrolyzed to recover phytohormone action. A family of metallopeptidase orthologues has been conserved in Plantae to help regulate auxin homeostatic levels during growth and development. This hydrolase family was recently traced back to liverwort, the most ancient extant land plant lineage. Liverwort's auxin hydrolase has little activity against auxin conjugate substrates and does not appear to actively regulate auxin. This finding, along with data that shows moss can synthesize auxin conjugates, led to examining another bryophyte lineage, *Physcomitrella patens*. We have identified and isolated three M20D hydrolase paralogues from moss. The isolated enzymes strongly recognize and cleave a variety of auxin conjugates, including those of indole butyric and indole propionic acids. These *P. patens* hydrolases not only appear to be "cryptic", but they are likely to have derived from soil bacteria through Horizontal Gene Transfer. Additionally, support is presented that the plant-type M20D peptidase family may have been universally lost from mosses after divergence from the common ancestor with liverwort.

Keywords *Physcomitrella patens* · Horizontal gene transfer · Auxin conjugate regulation · Amidohydrolase · Cryptic genes · Moss evolution

Introduction

Auxin can be found in all known Plantae species. This phytohormone has the ability to stimulate, promote, delay, or inhibit many physiological processes (Bandurski et al. 1995; Davies 1995), including gravitropism, phototropism, ethylene production, and cell elongation, division, and differentiation. Because it is so vital for growth and development, auxin homeostasis is closely controlled by the activities of biosynthesis, transport, conjugation, and molecular decay (Ljung et al. 2002; Korasick et al. 2013; Kasahara 2016).

Conjugated indole acetic acid (IAA), the most common form of auxin, is commonly believed to be non-functioning (Ludwig-Müller 2011). Conjugates come in two forms, bound to either one or more amino acids or ester-linked to sugar(s). These two conjugate types are found in assorted tissues of all Plantae, from bryophytes through angiosperms (Sztein et al. 1999, 2000). Although older studies suggest that a majority of IAA in a plant is stored in the conjugated form (Bandurski et al. 1995; Campanella et al. 1996), more recent work (Novak et al. 2012; Yu et al. 2015) suggests that endogenous levels of auxin conjugates are not as high as previously estimated. Free, functioning auxin is obtained by hydrolyzing the conjugate from the indole ring and carboxyl side-chain of the phytohormone. However, some auxin

Electronic supplementary material The online version of this article (https://doi.org/10.1007/s00344-019-09945-6) contains supplementary material, which is available to authorized users.

✉ James J. Campanella
James.campanella@montclair.edu

[1] Department of Biology, Montclair State University, 1 Normal Avenue, Montclair, NJ 07043, USA

[2] Department of Biology and Horticulture, Bergen Community College, 400 Paramus Rd, Paramus, NJ 07652, USA

[3] Institute of Botany, Technische Universität Dresden, 01062 Dresden, Germany

conjugates (IAA-Glutamate and IAA-Aspartate) have been found in *Arabidopsis* to be chemical "dead-ends" that are not hydrolyzed and employed as a degradation pathway (Sauer et al. 2013).

There is support that auxin amidohydrolases first evolved in photosynthetic bacteria, eventually becoming conserved in charophytic algae, which was the progenitor lineage of all terrestrial plants (Hori et al. 2014; Campanella et al. 2018). However, note that a parallel and independent evolutionary path emerged for amidohydrolases in soil bacteria. For example, an IAA-Aspartate amidohydrolase, that bears a striking homology to AtILR1 (*Arabidopsis thaliana IAA-leucine Resistant*), was isolated from *Enterobacter agglomerans* (Chou et al. 2002). Additional highly plant-like hydrolases have been characterized from *Arthrobacter ilicis* (Leong et al. 2009) and *Pseudomonas* (Rowsell et al. 1997). All these bacterial hydrolases evolved to parallel M20D peptidase evolution, including a structural penchant for manganese ion binding. These bacterial correspondences may support the long-held theory among protein evolutionary biologists that there are a limited number of conditions for constructing certain types of enzymes.

The recent isolation and characterization of an auxin amidohydrolase from the oldest land plant lineage known, liverwort (Wellman et al. 2003), illuminated the evolution of this family of enzymes in tracheophytes. Evidence was presented, based on phylogenetics and structural homology, that the only MpILR1 gene from liverwort was the ancestral genetic precursor to all tracheophyte auxin amidohydrolases (Campanella et al. 2018). However, what remained unanswered was where the other bryophytes might fit into this molecular evolutionary model. Ludwig-Müller et al. (2009a) proposed moss might have diverged as a "dead-end" in terms of auxin conjugate hydrolysis. There is general agreement that, although mosses are able to produce auxin conjugates, up until now no evidence for active auxin conjugate hydrolysis has been detected (Sztein et al. 1999, 2000; Cooke et al. 2002; Ludwig-Müller et al. 2009b).

Liverwort shows strong evidence of being a regulatory dead-end since the MpILR1 hydrolase demonstrates very little activity against auxin conjugate substrates (Campanella et al. 2018). That observation raises the question of how evolution of this pathway occurred in moss. Liverworts, hornworts, and mosses are thought to have evolved 50–75 million years before the emergence of the ancestral lineage of present-day tracheophytes (Ligrone et al. 2012). Additionally, mosses and hornworts appear to have diverged from a shared predecessor anywhere from 15 to 20 million years after liverwort first evolved (Qiu et al. 2006, 2007; Shen et al. 2017).

Motivated to determine if moss has a single, semi-active auxin amidohydrolase like liverwort, we probed the genome of *Physcomitrella patens* with in silico homology searches to detect orthologues for MpILR1. We were surprised to identify four putative homologues of the M20 peptidase family in *P. patens*, because we expected no more than the one hydrolase observed in liverwort (Campanella et al. 2018). Three of the four hydrolases (PpIAR32, PpIAR33, and PpIAR34) (*Physcomitrella patens IAA-Aspartate Resistant*) were verified as being part of the moss genome, while one is presumably a contaminant. In this paper, we characterize the enzymatic nature of these three auxin amidohydrolases, examine evidence for their evolutionary origin, and suggest what implications those origins have on the evolution of active auxin conjugate hydrolysis in tracheophytes.

Materials and Methods

Detection of Moss Hydrolase Homologues

The liverwort orthologue *MpILR1* DNA sequence (Campanella et al. 2018) was employed in BLAST analyses (Altschul et al. 1990) of the *P. patens* genome (v2.5) (Zimmer et al. 2013) on the Phytozome Web site (http://www.phytozome.jgi.doe.gov). Four orthologues were detected by this investigation (Phpat.1Z030500.1, Phpat.1Z047400.1, Phpat.1Z039000.1, and Phpat.1Z023000.1). Successive BLAST searches on GenBank with these newly discovered moss sequences indicated that they had the greatest sequence similarity to the IAR-like hydrolases, so they were dubbed PpIAR31, PpIAR32, PpIAR33, and PpIAR34. Default search parameters were utilized with BLAST. In version 3.3 of the genome, the designations were as follows: PpIAR32: Pp3s46_160V3.1; PpIAR33: Pp3s34_741V3.1; PpIAR34: Pp3s32_480V3.1.

Genomic PCR Probing

Moss whole DNA extraction employed approximately 30 mg of dried *P. patens* tissue. Extraction was performed with the QIAGEN DNeasy Plant kit using the company's directions (QIAGEN Corp., Hilden, Germany). DNA concentration was ascertained with a NanoDrop ND-1000 Spectrophotometer (Thermo Fisher Scientific Inc., Waltham, Massachusetts), and genomic DNA stored at − 20 °C.

Two replicates with each set of primers and two controls using commercial 18S primers were prepared—so four reaction tubes total were set up for each of the hydrolase genes examined. Two reactions contained 5 µl of moss DNA, 1 µl of each appropriate primer (Supp. Table 1), 12.5 µl of Mastermix (Denville Scientific Inc., Holliston, Massachusetts), and 5.5 µl of sterile DI water—equaling a total volume of 25 µl. The second two reactions contained 5 µl of moss sample 1 DNA, 1 µl of universal 18S primers (QuantumRNA

Classic II 18S Internal Standard, Thermo Fisher Scientific Inc.), 12.5 µl of Mastermix, and 6.5 µl of sterile DI water.

All primers were constructed by Invitrogen (a division of Thermo Fisher Scientific Inc.). Samples were preheated in the thermocycler [Eppendorf Mastercycler ep gradient S (Eppendorf, Hauppauge, New York)] for 1 min at 95 °C and subsequently treated to the following program for 40 cycles: 95 °C for 45 s, 54–56 °C for 45 s, 72 °C for 60 s. Annealing temperatures varied by primer set (Supp. Table 1).

PCR products were electrophoresed in 1 × TAE on 2% agarose gels (Marine BioProducts Inc., B.C., Canada) for 30 min, stained with stock ethidium bromide (Thermo Fisher Scientific Inc.), and then analyzed by UV Transilluminator (Ultra-Lum Inc., Paramount, California) with digital photography.

RNA Extraction and RT-PCR

Moss whole RNA extraction employed approximately 10 mg of dried *P. patens* gametophytic tissue. Extraction was performed with the Norgen Plant/Fungal Total RNA Purification Kit using the company's directions (Norgen Biotek Corp., Ontario, Canada) and after purification treated 15 min at 20 °C with 2 units DNase (Promega Corp, Madison, WI). Total RNA concentration was ascertained with a NanoDrop ND-1000 Spectrophotometer (Thermo Fisher Scientific Inc., Waltham, MA), and RNA stored at − 70 °C.

The primers employed to amplify mRNA of PpIAR32, PpIAR33, and PpIAR34 for expression analysis are listed in Supplementary Table 1. For the expression analyses, single 150-ng, 25-µl reactions were carried out in RNase-free 0.2-ml microfuge tubes using an Mx3000p Real Time Thermocycler (Stratagene, La Jolla, CA). The SuperScript IV One-Step RT-PCR (Thermo Fisher Scientific Inc., Waltham, MA) was employed according to the manufacturer's instructions to amplify the specific cDNA of PpIAR32, PpIAR33, and PpIAR34. The reverse transcriptase reaction was incubated at 50 °C for 15 min, followed by 98 °C for 3 min. The PCR step was performed for 40 cycles at the following times and temperatures: 10 s at 95 °C, 10 s at 56 °C, and 30 s at 72 °C. This program was completed by a final extension for 5 min at 72 °C. 18S RNA was used as an expression control (primers: QuantumRNA Classic II 18S Internal Standard, Thermo Fisher Scientific Inc.). Expression analysis was analyzed by 1.5% agarose gel electrophoresis in 1 × TAE for 30 min at a constant 150 V.

Cloning and Construction

Synbio Technologies (Monmouth Junction, New Jersey) synthesized the DNA sequences of PpIAR32, PpIAR33, and PpIAR34 for our use. *PpIAR32* was designed to be ligated in-frame into the expression vector PetBlue2 (Novagen Corp. (EMD Chem. sub.), Madison, Wisconsin). *PpIAR33* and PpIAR34 were designed as an entire cassette. The cassette included a Shine-Dalgarno sequence in the 5′ untranslated region with a T7 inducible IPTG promoter just upstream.

The *PpIAR32* insert was ligated into the *Bam*HI site of a pUC57 plasmid in Synbio Tech. We amplified the PpIAR32 fragment from the pUC57 plasmid using PCR (F-primer: 5′-GTTCATGCAAGCATTGGTTT-3′, R-primer: 5′-GATCCCTGACCCATTTTTCA-3′) with the following 40-cycle program: 95 °C for 45 s, 56 °C for 45 s, 72 °C for 60 s (primers from Invitrogen Corp., a division of Thermo Fisher Scientific Inc.). The fragment was blunt-end ligated into the EcoRV site of the PetBlue2 plasmid using the directions of the kit manufacturer (Novagen Corp.). We utilized heat shock to transform the ligation mixture into NovaBlue *E. coli* cells (Sambrook et al. 1989).

The *PpIAR33 and* PpIAR*34* constructs were dissolved in 1 ml sterile water to give ~ 40 ng/µl concentration and 1 µl used directly for transformation into NovaBlue Cells.

Transformants were all selected on Luria–Bertani media (50 µg/ml ampicillin) and blue–white selection (Sambrook et al. 1989). Alkaline lysis was employed to isolate plasmids from transformants (Sambrook et al. 1989). DNA sequencing of the insert regions was done by manufacturer's instructions, utilizing BigDye Terminator version 3.0 with an ABI model 3730 DNA Analyzer (Applied Biosystems Inc., CA).

Enzyme Preparation from *E. coli* and Hydrolase Enzyme Assays

MpIAR32, MpIAR33, and MpIAR34 cultures were grown 16–18 h at 37 °C in 5 ml Luria–Bertani medium (100 µg/ml ampicillin). For gene induction, 2 ml was transferred from each culture into a flask with 50 ml Luria–Bertani culture medium (100 µg/ml ampicillin, 1 mM IPTG). Untransformed NovaBlue control cells were grown without added IPTG. We performed induction of transgene expression for 4 h with continuous shaking of the cultures.

We prepared enzymes as in our previous studies by sonic disruption and lysis of cells (Campanella et al. 2003a, 2004, 2008). Protein extracts (100 µl employed per assay) were either stored at − 80 °C long term or directly utilized for the enzyme assays.

The methods of Campanella et al. (2008) were followed precisely for the performance of enzyme assays for auxin conjugate hydrolysis. IAA-amide conjugates employed were: IAA-Aspartate, -Alanine, -Glycine, -Leucine, -Isoleucine, -Phenylalanine, and -Valine (Sigma-Aldrich, Saint Louis, Missouri). We also utilized IBA-Alanine (Sigma-Aldrich) and IPA-Alanine (Campanella et al. 2008). The HPLC protocol of Campanella et al. (2003a) was used to analyze final hydrolysis test samples.

Experiments were replicated four to six times employing the various enzyme preparations. We then calculated the mean for these independent experiments ± the standard error. We utilized the uninduced cultures as controls and estimated enzymatic activity in picomoles of IAA, IBA, or IPA released from the IPTG-induced cultures minus the values acquired in non-expressing controls.

Exogenous Treatment of Auxin Conjugates to Gametophores of *Physcomitrella patens*

For each *P. patens* sample between 200 and 500 mg fresh weight were used. Two discrete experiments were executed with three biological replicates each, separately incubated with the respective conjugate.

The gametophores were pre-cultivated for 4 weeks on agar plates with KNOP medium (Ludwig-Müller et al. 2009b). The gametophores were then transferred to 6-well plates with 10 ml liquid KNOP medium and 100 µM of the respective conjugate or without conjugate. Conjugates used were IAA-Ala, IAA-Gly, IBA-Ala, IPA-Ala. For each condition, one well was used. The moss plants were incubated 24 h at RT° with continuous shaking at 100 rpm. The gametophores were removed for harvesting from the medium and completely rinsed with water. Subsequently, they were dried on filter paper and the fresh weight determined.

The plant material was homogenized using 2 ml isopropanol:1% acetic acid (95:5, v/v) and sea-sand. During extraction, the heavy isotope labeled standards were added to all samples 100 ng $^{13}C_6$-IAA (Ehrenstorfer GmbH, Germany) and to the samples incubated with the IBA conjugate 50 ng $^{13}C_8/^{15}N_1$-IBA (a gift from Dr. Jerry D. Cohen; Barkawi et al. 2008). The extracts were incubated under continuous shaking for 1.5 h (4 °C, 800 rpm) and then centrifuged for 10 min and 13,000×*g* at 8 °C. The supernatant was removed and evaporated to the aqueous phase under a stream of N_2. To better adjust the pH, we added 500 µl H_2O to each sample and adjusted with 1 M HCl. Samples were extracted two times with two volumes of ethyl acetate. The organic phases were removed under a stream of N_2 and combined. The organic phases were then evaporated to dryness and resuspended in 200 µl methanol. For methylation, 200 µl trimethylsilyldiazomethane (Sigma-Aldrich, Germany) diluted 1:10 in diethylether was added and incubation was performed for 30 min at room temperature (Geilfus et al. 2018). The samples were incubated for 30 min at RT and then evaporated to dryness under N_2. The sample was finally dissolved in 50 µl ethyl acetate for GC–MS analysis, and 1 µl was injected in a Varian Saturn 2100 ion-trap mass spectrometer using electron impact ionization at 70 eV, connected to a Varian CP-3900 gas chromatograph equipped with a CP-8400 autosampler (Varian, Walnut Creek, CA, USA). Injection was with splitless mode (splitter opening 1:100 after 1 min) onto a Phenomenex (Aschaffenburg, Germany) ZB-5 column (30 m × 0.25 mm × 0.25 µm) employing helium carrier gas at 1 ml/min. The temperature program was as described in Campanella et al. (2008).

Auxin contents were calculated using the isotope dilution equation (Cohen et al. 1986) with m/z 130 and 136 for IAA and m/z 130 and 139 for IBA. Because no heavy labeled standard for IPA was available to us, the calculation was an estimation based on the labeled IAA standard.

Codon Usage Analysis

We took DNA coding sequences of auxin conjugate hydrolases from Archaea, Eubacteria, and eukaryotes (algae, bryophytes, tracheophytes) and performed a principal coordinate analysis for codon usage in open reading frames. The program EMBOSS CUSP (Lu et al. 2005) was applied to determine the relative abundance values. With this abundance data, a dissimilarity matrix (Bray and Curtis 1957) was calculated by Vegan (Oksanen et al. 2016). The principal coordinate analysis was then implemented using classical multidimensional scaling (R Core Team 2014; Gower 2015), and the final plot generated using *ggplot2* (Wickham 2009).

Global Alignment and Phylogenetic Tree Construction

MatGAT v1.1 (Campanella et al. 2003b) in default configuration was used to generate the amino acid sequence similarity matrix of the amidohydrolase homologues.

Phylogenetic tree construction was implemented using CLUSTAL X v1.81 (Thompson et al. 1997) in default mode. Amino acid sequences of hydrolase homologues were aligned by CLUSTAL X, and neighbor-joining values ascertained (1000 bootstraps applied) (Saitou and Nei 1987; Felsenstein 1985). While CLUSTAL generated the genetic branch distances and bootstrap values, the radial phylogram itself was visualized by TreeView (Page 1996).

Accession Numbers

The Phytozome accession numbers for the *P. patens* hydrolase genes *(PpIAR32, PpIAR33, and PpIAR34)* are Pp3s46_160V3.1, Pp3s34_741V3.1, and Pp3s32_480V3.1. The following GenBanked genes were employed in the phylogenetic analyses: liverwort (OAE20874.1), *K. flaccidum* (GAQ79540), *Arabidopsis* (NP_175587.1), fern (XP_002981614.1,), spruce (EF085410.1), *Brevibacillus* (WP_092267846, WP_055746795), *Bacillus simplex* (WP_076372044), *Lysinibacillus* (WP_054610332), *Bacillus* (WP_049662221), rice (XP_015621783), *Enterobacter agglomerans* (AF006687), *Arthrobacter ilicis* (EU400596).

Results

The PpIAR31 Gene Cannot be Detected in the *P. patens* Genome

Our initial study of Rensing et al.'s (2008) v1.1 moss genome database made us aware that bacterial DNA contamination could account for the presence of "plant" amidohydrolases we detected. To assure ourselves that we were studying moss genes, we designed PCR primers for unique regions of the PpIAR31, *PpIAR*32, *PpIAR*33, and *PpIAR*34 genes so that they could be easily identified. We performed PCR using moss nuclear DNA as the template and found that the amplified fragments of PpIAR32, *PpIAR*33, and *PpIAR*34 could be detected, but not that of PpIAR31 (Supp. Fig. S1). The 18S DNA positive controls were seen with all the samples. Negative bacterial controls were included, employing primers derived from the auxin amidohydrolases of *E. agglomerans* (AF006687) and *A. ilicis* (EU400596). No PCR amplification was detected in moss DNA from these negative controls (data not shown).

Further evidence that PpIAR31 was a genomic sequencing artifact in the moss v2.1 was observed in the newest v3.3 genome. The Lang et al. (2018) version 3.3 of the *P. patens* genome was not available; at the time this research was first initiated and PpIAR31 was first detected. We employed the Phytozome Web site to perform a BLAST search using the PpIAR31 DNA sequence with v3.3, but we could no longer detect the original sequence from the earlier v2.1.

Evidence for Horizontal Gene Transfer in the PpIAR Family

There are several strands of evidence that suggest that PpIAR32, *PpIAR*33, and *PpIAR*34 all originated in bacteria by HGT. Initially, we employed principal coordinate analysis of codon usage (Fig. 1). On the PCoA, the bryophyte (moss) genes intersect strongly with Eubacteria, less so with Archaea, and barely with Plantae. These results suggest that these isolated moss genes use prokaryotic codons more frequently than those of eukaryotes.

Further, we analyzed the intronic structure of the three genes using the Phytozome BLAST software. However, PpIAR32, *PpIAR*33, and *PpIAR*34 have *no* introns present in their genomic sequences. These data are in direct contrast to the liverwort MpILR which has a genomic structure of five exons and four introns that has been conserved all the way through angiosperms (Campanella et al. 2018). Again, the lack of introns supports a bacterial origin for the moss hydrolases.

We next performed a global amino acid alignment using MatGAT v1.1 (Campanella et al. 2003b) and generated a similarity matrix to compare the structure of PpIAR32, *PpIAR*33, and *PpIAR*34 to an orthologous group of eubacterial and plant hydrolases (Supp. Fig. S3). PpIAR32 showed strongest similarity to hydrolases from *Bacillus simplex* (48.2%) and *Lysinibacillus* (46.5%)—no plant hydrolase had a higher homology than 30% (Supp. Fig. S3). The same pattern was observed with PpIAR33 with similarity values of ~ 79% with *Brevibacillus sp1* and *sp2* orthologues. The *Arthrobacter* IAA-Alanine hydrolase (Leong et al. 2009) shows a more distant similarity to PpIAR33 at 51.4%. PpIAR34 demonstrates a high similarity value of 93.8% with the *Bacillus* enzyme (Supp. Fig. S3). Again, no plant similarity values were as high as these, suggesting a stronger homology to eubacteria than to eukaryotes.

Finally, an unrooted, neighbor-joining phylogram was generated utilizing amino acid sequence data for each moss hydrolase (Fig. 3). The non-rooted, radial tree shows the hydrolases separating into two clades. The eukaryotic clade includes angiosperms, spruce, algae, fern, and liverwort. The prokaryotic clade includes all three moss hydrolases (Fig. 3). High bootstrap values of primarily over 70% help to support the branch relationships. This last analysis supports all the others and lends high probability that PpIAR32, *PpIAR*33, and *PpIAR*34 all arose from HGT.

The PpIAR Hydrolase Family has Strong Activity Against a Variety of Auxin Conjugates

In vitro auxin conjugate hydrolysis tests were conducted with all of the heterologously expressed moss proteins to establish substrates and potential enzymatic activity (Table 1). All three amidohydrolases recognized a variety

Table 1 Enzyme/substrate specificity of the *P. patens* auxin hydrolases

Substrate	PpIAR32	PpIAR33	PpIAR34
IAA-Alanine	20.9 + 7.6	95.5 + 82.0	313.3 + 11.7
IAA-Glycine	24.0 + 2.3	27.1 + 3.4	0
IAA-Aspartate	0	0	0
IAA-Leucine	0	0	234.4 + 64.7
IAA-Isoleucine	0	0	446.9 + 138.7
IAA-Valine	10.1 + 6.6	0.349 + 0.27	0
IAA-Phenylalanine	0	0	322.7 + 64.0
IPA-Alanine	150.5 + 52.5	229.0 + 132.4	0
IBA-Alanine	10.8 + 2.9	69.7 + 24.5	2043.7 + 263.1

All hydrolase values are expressed as picomoles of auxin released per minute per milliliter (average from 4 to 7 replicate experiments) plus or minus the standard error. Untransformed *E. coli* (NovaBlue) cells were employed as negative hydrolysis controls

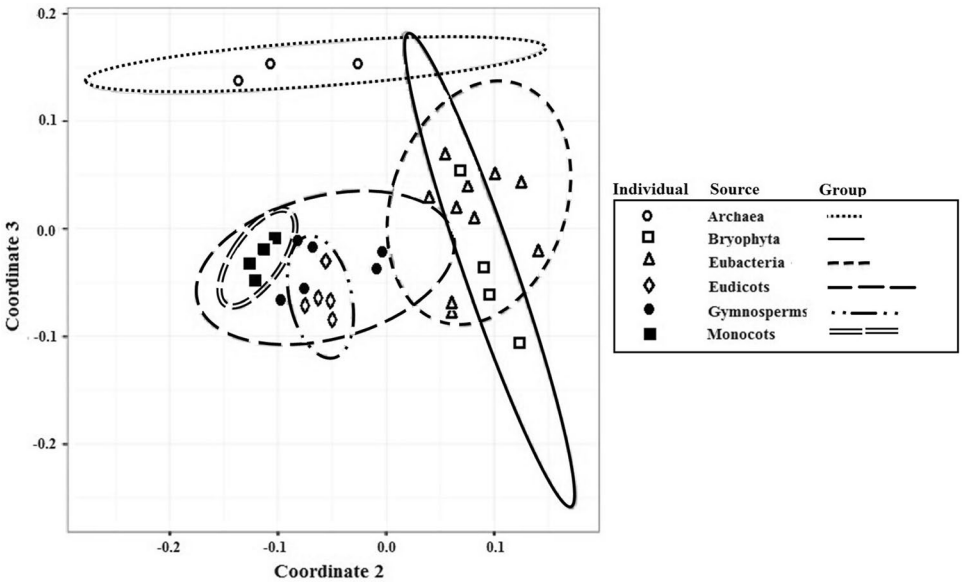

Fig. 1 Principal coordinate analysis of codon usage to determine if the moss hydrolases have bacterial origins and are likely to have come from Horizontal Gene Transfer. The two-dimensional plot was created using ggplot2 (Wickham 2009)

Table 2 Auxin released in Plantae from exogenous conjugate treatment

Conjugate	Average release auxin (ng/g fr. wt + standard dev.)[a]
Control	12.89 ± 4.18
IAA-Alanine	60.63 ± 4.55
IAA-Glycine	74.15 ± 22.39
IBA-Alanine	57.17 ± 23.64
IPA-Alanine	32.78 ± 25.07

[a]For each sample, between 200 and 500 mg fresh weight was used. Two separate experiments were performed with three biological samples each, which were separately incubated with the respective conjugate

of IAA conjugates, as well as IBA and IPA conjugates. PpIAR32 and PpIAR33 converted IAA-Ala, -Gly, and -Val, as well as IPA-Ala and IBA-Ala to the free auxin. PpIAR34 differed from the two paralogues and recognized IAA-Ala, -Leu, -Ile, -Phe, and IBA-Ala. The hydrolytic abilities of PpIAR32 and *PpIAR*33 were completely redundant, while PpIAR34 seemed to hydrolyze those conjugates not recognized by the other two enzymes.

Physcomitrella patens can Hydrolyze Several Different Conjugates In Vivo and Release Auxin

Finally, we examined the ability of the *P. patens* gametophytic tissues to hydrolyze conjugates in vivo (Table 2). The level of auxin released from the exogenously treated plants was anywhere between ~ 2.6- and 6.2-fold greater than the mock-treated controls. IAA-Glycine seemed to be most prone to degradation at 74.15 ± 22.39 ng/g fresh weight of moss gametophytic tissues. Sporophytic tissues were not analyzed.

Discussion

Auxin Regulation and the "Dead-End" Nature of Moss Hydrolases

Horizontal Gene Transfer has been observed innumerable times in the last decade across the whole Plantae kingdom (Bock 2009; Yue et al. 2012; Fang et al. 2017). The HGT process appears to be common among plants as a form of diversifying the genome by expanding the gene pool. This process of gene movement across species is thought to drive genomic and phenotypic alteration and augment reproductive fitness. Yue et al. (2012) identified 57 families of over 900 genes assimilated from viruses, fungi, and Eubacteria into the *P. patens* genome. The majority of HGT sequences identified in this moss were derived from miscellaneous bacterial lineages.

We have concluded that the auxin amidohydrolases identified in the *P. patens* genome (PpIAR32, *PpIAR*33, and *PpIAR*34) have their evolutionary source in HGT and not in earlier plant lineages. We base this conclusion on the phylogenetic evidence (Figs. 2, 3), codon usage analysis (Fig. 1), and the lack of conserved intronic structure in the three moss hydrolases. In every instance, the moss hydrolases appear to be more similar to eubacterial genes than eukaryotic genes.

Because these hydrolase genes apparently have their source in HGT, we do not see any evidence that they are required for the homeostatic regulation of auxin in moss. *P. patens* does not appear to be in the evolutionary line of auxin amidohydrolases that Campanella et al. (2018) suggested

		1	2	3	4	5	6	7	8	9	10	11	12	13	14	15
1.	PpIAR32															
2.	PpIAR33	36.1														
3.	PpIAR34	22.9	48.0													
4.	*Enterobacter*	25.7	40.6	40.1												
5.	*Arthrobacter*	26.7	51.4	45.4	45.4											
6.	*Brevibacillus sp.1*	44.7	**79.4**	48.4	43.3	52.8										
7.	*Brevibacillus sp.2*	40.8	**79.0**	47.9	45.4	55.8	89.5									
8.	*Bacillus simplex*	**48.2**	32.9	32.3	36.1	33.8	30.4	34.4								
9.	*Lysinibacillus*	**46.5**	31.8	30.9	30.7	33.3	32.0	33.5	86.3							
10.	*Bacillus*	22.1	48.0	**93.8**	39.7	44.9	47.9	48.5	31.4	30.1						
11.	*Arabidopsis*	27.0	47.3	38.9	45.0	50.2	45.2	49.5	35.7	37.1	38.5					
12.	Fern	24.9	50.9	43.2	44.0	54.8	51.4	53.8	33.3	34.3	41.7	61.8				
13.	Spruce	30.8	42.9	36.1	43.3	43.7	44.3	45.6	35.1	37.4	36.8	64.9	61.1			
14.	Rice	23.2	43.9	37.7	37.6	43.0	45.3	45.1	30.2	32.8	37.2	51.1	54.8	52.5		
15.	Liverwort	30.8	46.6	37.4	41.5	46.1	47.4	47.2	35.9	37.0	35.9	60.8	61.2	68.5	47.8	
16.	Algae	27.8	48.0	39.9	44.2	48.7	46.2	49.8	32.7	36.2	40.6	63.0	57.0	58.8	48.9	62.2

Fig. 2 Similarity matrix comparing the *P. patens* hydrolase amino acid protein sequence homology to a panel of Eubacterial and Plantae orthologues. The matrix was generated with MatGAT v1.1 by using the default values for protein analysis. Values in bold indicate high levels of similarity for the three moss hydrolases

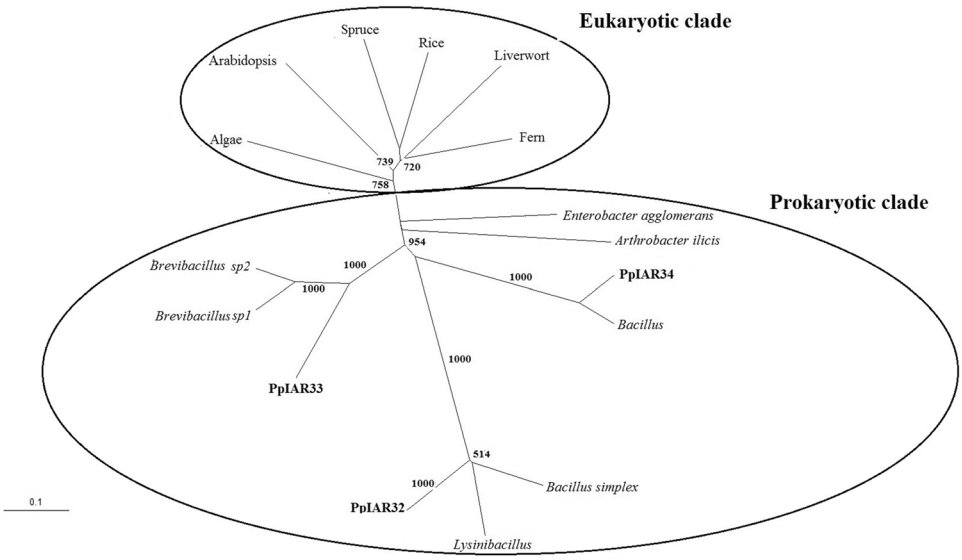

Fig. 3 A non-rooted, radial phylogram of the M20/M25/M40 peptidase protein family members. CLUSTAL X was employed for alignment, and bootstrapping was performed 1000 times. The moss hydrolases in the prokaryotic clade are indicated by bold

began in charophytic algae. Even though PpIAR32, *PpIAR*33, and *PpIAR*34 are capable of active hydrolysis, none of the hydrolases that we identified in the moss genome are expressed in any tissues. For the *P. patens* genome v3.3, Lang et al. (2018) performed expression analyses under 30 different environmental conditions in all tissues, and none of these hydrolases are expressed under any circumstance (Supp. Fig. S2). We performed control BLAST searches with *Arabidopsis* sequences of actin, phytochrome C, and GH3 to quality test the *P. patens* v3.3 expression analysis and found all three conserved genes expressed in the cDNA library (data not shown). Additionally, we performed our own RT-PCR expression analysis with each moss amidohydrolase, and we could detect no expression of these genes in gametophytic tissues (Supp. Fig. S3).

We conclude that the transference of these three amidohydrolases had little impact on auxin conjugate regulation in moss. To have any effect on auxin regulation, they would need to have been actively expressed. Because they are not expressed, these genes are essentially non-functional and the paralogues have become "passengers" in the moss genome, or what is sometimes referred to as "cryptic" genes.

Although *P. patens* is the lone moss species whose complete genome is presently accessible for study, we can make some tentative statements about the *Sphagnum fallax* (peat moss) genome v0.5 that is available on the Phytozome Web site, as well as a number of other moss species. We performed Phytozome BLAST searches with *Arabidopsis* sequences of AtILR, AtIAR, actin, phytochrome C, and GH3 to probe for amidohydrolases and positive controls in the *S. fallax* genome v0.5. We detected no homologues for the M20D peptidase genes in peat moss, although the positive control searches for the three conserved genes identified orthologues for each (data not shown).

In addition to the sphagnum genomic analysis, we performed BLAST searches on moss transcriptome data from the 1000 plants Web site (onekp.com). The 1000 plants Web site (Matasci et al. 2014) stores transcriptomic data from 41 moss species. We employed the MpILR1 gene from liverwort as well as the AtILR1 *Arabidopsis* hydrolase as BLAST probes. We detected no M20D peptidase orthologues in any of the 41 species probed using both DNA and protein sequences.

Our results therefore suggest strongly that the charophytic-derived M20D peptidase homologue may have been universally lost from mosses after divergence from the common ancestor with liverwort. The lack of any prokaryote-like amidohydrolase orthologues in the moss species probed in the 1000 plants Web site also suggests that *P. patens* may have been unique among mosses to undergo HGT and restore peptidases back into its genome. These results support that moss is indeed a "dead-end" for auxin conjugate hydrolysis and that the clade may be unique among all Plantae to not possess this regulatory plant-type hydrolase even in the "low functioning" state of the liverwort MpILR1 (Campanella et al. 2018).

HGT Timing and Hydrolytic Activity in *P. patens*

It is difficult to propose at what point in evolution the amidohydrolase HGT took place from bacteria to *P. patens*. Because this species is between 425 and 450 million years old, the transfer could have occurred anywhere from its initial divergence to relatively modern times—especially given that we are probably not talking about a single event. Note that since PpIAR32 (Fig. 2) bears such low similarities to the others at 36% (PpIAR33) and 22.9% (PpIAR34), they are unlikely to have arisen from gene duplication from *PpIAR*32. However, it is possible that PpIAR33 arose from PpIAR34 from gene duplication (or vice versa) because the similarity between those two genes is much higher at 48.0%. Therefore, there were probably at least two HGT events.

The two to three transfer events could have taken place with potentially millions of years between each. However, the lack of observed bacterial orthologues for this gene family in tracheophytes suggests that they were likely transferred more recently in evolutionary time to *P. patens*, long after the common ancestor for moss and vascular plants. Another factor that suggests relatively recent HGT is that all three hydrolases retain their hydrolytic activity. If they remained tens of millions of years under neutral selection in the moss genome, they would most likely have lost activity through many random background mutations.

Whether the transfer from bacteria occurred early or more recently in evolutionary time, *P. patens*, and perhaps peat moss as well, appears to have differentially lost the "original" auxin amidohydrolase inherited from the common charophytic algal ancestor that it shares with liverwort (Hori et al. 2014). Although we find homologues for the *Klebsormidium flaccidum* amidohydrolase (GAQ79540.1) in liverwort, and tracheophytes starting with fern, we cannot find evidence of an orthologue for this gene in *P. patens*. If this "original" moss enzyme was lost and HGT eventually supplied new, though non-expressed hydrolase orthologues, we can initially conclude that Ludwig-Müller et al.'s (2009a) proposal that moss is a dead end for conjugate hydrolysis appears to be correct.

However, discounting the activity of these three amidohydrolases creates a difficulty in explaining our experimental observations. Exogenous treatment of *P. patens* tissues with auxin conjugates yielded detectable auxin hydrolysis and release. There are three possibilities to explain the observed in vivo hydrolysis.

First, it is conceivable that there is an uncharacterized, expressed enzyme in the moss genome that bears little homology to the M20D peptidases and hydrolyzed the exogenous auxin conjugates. Given that we and others (Bock 2009; Yue et al. 2012; Fang et al. 2017) have detected multiple HGT events in plants, it is feasible that an additional HGT event brought in a trans-specific enzyme to the *P. patens* genome, for example from virus or fungi, that we cannot detect by homology searches with plant genes.

Second, there may be additional M20D paralogues in *P. patens* that are expressed. This seems possible, but we have done extensive BLAST searches on *P. patens* v3.3 and found no other expressed amidohydrolases. However, a putative hidden paralogue may be undetectable because the v3.3 version may still be an incomplete reflection of the moss genome. In light of this hypothesis, Smolko et al. (2018) reported in a recent review the detection of at least one expressed amidohydrolase (Pp1s9535_1V6.1) in an unreleased v6.1 of the *P. patens* genome for which transcriptome data are available at the *Physcomitrella* eFP browser at bar.utoronto,com (Ortiz-Ramirez et al. 2016). In addition, modeling revealed that the v6.1 enzyme bears high homology to the *Arabidopsis* AtILL2 protein (*Arabidopsis thaliana ILR1-like*) (Smolko et al. 2018), indicating that it could be an active enzyme in Plantae. However, as seen in this present study, the v6.1 protein also has higher homology to bacterial sequences than to plant hydrolases. Our BLAST search of *P. patens* on Phytozome with the Pp1s9535_1V6.1 sequence did not appear in the Lang et al.'s (2018) v3.3 of the sequence database.

The third—least likely—possibility is that we are seeing background degradation, and the chemical milieu of our negative control buffer did not sufficiently complement that of the inside of the moss tissue in terms of pH, ion concentration, etc. to manifest similar background degradation. It may be that auxin conjugate degradation can also

occur within moss tissues because of specific chemico-physiological conditions and not just because of peptidases present.

Of course, it cannot be ruled out that very low expression, not detected by us or Lang et al. (2018), occurs that would lead to enough protein present to explain the basal levels of hydrolytic activities we see after incubation of plants with different IAA amide conjugates.

Although we cannot detect the charophytic-descendent of the auxin conjugate amidohydrolase gene in the *P. patens* genome, the ability to synthesize auxin conjugates for regulatory purposes appears to still be present. Ludwig-Müller et al. (2009b) found that the PpGH3 synthetases can produce: IAA-Ala, -Asp, -Gln, -Glu, -Gly, -Ile, -Leu, -Met, -Trp, -Val, and -Cys. *Physcomitrella* can even synthesize ester conjugate compounds (Ludwig-Müller et al. 2009b).

Although no one has examined *P. patens* to determine which auxin conjugate is the native product, the most likely of these compounds to be present in vivo may be IAA-Val, because this conjugate has been found commonly in several other moss species (Sztein et al. 1999). A more recent study from Drábková et al. (2015) examined conjugates present in a large number of bryophytes and found the most common moss conjugate was IAA-Aspartate at low concentrations. They concluded that liverworts prefer conjugation as a regulatory scheme while mosses favor degradation strategies to maintain homeostasis. This conclusion would also support the "dead-end" hypothesis.

Conclusion

Auxin conjugate degradation in *P. patens* appears to have diverged from the pathway beginning in algae and liverwort (Campanella et al. 2018). Tracheophytes and hornworts are thought to have a common ancestor, whereas mosses diverged at an earlier point (Ligrone et al. 2012; Shen et al. 2017). Both bryophyte lineages are thought to come from a common ancestor with liverwort. If hornworts and tracheophytes indeed have a common ancestor that diverged away from mosses, then we may find the same conserved hydrolase in hornwort (Fig. 4).

It is possible that mosses, when they diverged away from the hornwort/tracheophyte line, lost this gene (Fig. 4). We will not know how pervasive that loss may have been until we look at the genomes of other moss species. In addition, we need to examine hornwort with the same physio-evolutionary questions that we have considered here. Does hornwort retain the auxin hydrolase conserved in tracheophytes, does this putative hornwort enzyme have greater hydrolytic activity than MpILR1, and is regulation by auxin conjugate hydrolysis an active process in hornwort?

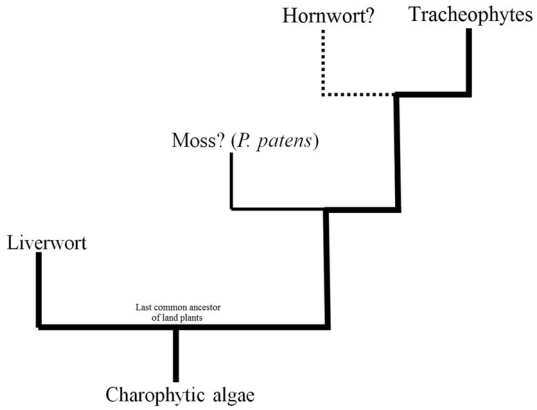

Fig. 4 Proposed model of how the conserved M20 aminopeptidases evolved from algae up into Plantae. The dark, thick contiguous line indicates the diverging path through which we believe the gene family has evolved. The dotted line to hornwort indicates a lack of information on the genome. The thinner line into moss indicates that other than *P. patens*, the process of molecular evolution of this family is not clarified in this group of bryophytes. The model is based on that of general bryophyte evolution from Ligrone et al. (2012)

Acknowledgements The authors would like to thank Dirk Vanderklein and Scott Kight for their advice and encouragement. We would also like to thank Lisa Campanella for the help in revising this manuscript. The technical help of Adam Parker of MSU and Sabine Rößler, TU Dresden, is gratefully acknowledged. This work was supported by a Margaret and Herman Sokol Fellow Award, #07A. The authors of this article have no conflicts of interest.

References

Altschul SF, Gish W, Miller W, Myers EW, Lipman DJ (1990) Basic local alignment search tool. J Mol Biol 215(3):403–410

Bandurski RS, Cohen JD, Slovin JP, Reinecke DM (1995) Auxin biosynthesis and metabolism. In: Davies PJ (ed) Plant hormones, 2nd edn. Kluwer Academic Publishers, Boston, pp 39–65

Barkawi LS, Tam Y-Y, Tillman JA, Pederson B, Calio J, Al-Amier H, Emerick M, Normanly J, Cohen JD (2008) A high-throughput method for the quantitative analysis of indole-3-acetic acid and other auxins from plant tissue. Anal Biochem 372:177–188

Bock R (2009) The give and take of DNA: horizontal gene transfer in plants. Trends Plant Sci 15(1):11–22

Bray JR, Curtis JT (1957) An ordination of the upland forest of Southern Wisconsin. Ecol Monogr 27:325–349

Campanella JJ, Ludwig-Müller J, Town CD (1996) Isolation and characterization of mutants of *Arabidopsis thaliana* with increased resistance to growth inhibition by indoleacetic acid amino acid conjugates. Plant Physiol 112:735–745

Campanella JJ, Ludwig-Müller J, Bakllamaja V, Sharma V, Cartier A (2003a) ILR1 and sILR1 IAA amidohydrolase homologues differ in expression pattern and substrate specificity. Plant Growth Regul 41:215–223

Campanella JJ, Bitincka L, Smalley JV (2003b) MatGAT: an application that generates similarity/identity matrices using protein or DNA sequences. BMC Bioinform 4:29

Campanella JJ, Olajide A, Magnus V, Ludwig-Müller J (2004) A novel auxin conjugate from wheat with substrate specificity for longer side-chain auxin amide conjugates. Plant Physiol 135:2230–2240

Campanella JJ, Smith SM, Leibu D, Wexler S, Ludwig-Müller J (2008) The auxin conjugate hydrolase family of *Medicago truncatula* and their expression during the interaction with two symbionts. J Plant Growth Regul 27(1):26–38

Campanella JJ, Kurdach K, Bochis J, Smalley JV (2018) Evidence for exaptation of the *Marchantia polymorpha* M20D peptidase MpILR1 into the tracheophyte auxin regulatory pathway. Plant Physiol 177(4):1595–1604

Chou J-C, Mulbry WW, Cohen JD (2002) N-carbobenzyloxy-D-aspartic acid as a competitive inhibitor of indole-3-acetyl-L-aspartic acid hydrolase of *Enterobacter agglomerans*. Plant Growth Regul 37:241–248

Cohen JD, Baldi BG, Slovin JP (1986) $^{13}C(_6)$-[benzene ring]-indole-3-acetic acid: a new internal standard for quantitative mass spectral analysis of indole-3-acetic acid in plants. Plant Physiol 80:14–19

Cooke TJ, Poli DB, Sztein AE, Cohen JD (2002) Evolutionary patterns in auxin action. Plant Mol Biol 49:319–338

Davies PJ (1995) Plant hormones: physiology, biochemistry and molecular biology. Klewer Academic Publishers, Dordrecht

Drábková LZ, Dobrev PI, Motyka V (2015) Phytohormone profiling across the bryophytes. PLoS ONE 10(5):e0125411

Fang H, Liexiang H, Rujia C, Pengcheng L, Shuhui X, Enying Z, Wei C, Liu L, Youli Y, Guohua L et al (2017) Ancestor of land plants acquired the DNA-3-methyladenine glycosylase (MAG) gene from bacteria through horizontal gene transfer. Sci Rep 7:9324

Felsenstein J (1985) Confidence limits on phylogenies: an approach using the bootstrap. Evolution 39:783–791

Geilfus C-M, Ludwig-Müller J, Bárdos G, Zörb C (2018) Early response to salt ions in maize (*Zea mays* L.). J Plant Physiol 220:173–180

Gower JC (2015) Principal coordinates analysis. Wiley StatsRef: Statistics Reference Online, pp 1–7

Hori K, Maruyama F, Fujisawa T, Togashi T, Yamamoto N, Seo M, Sato S, Yamada T, Mori H, Tajima N et al (2014) *Klebsormidium flaccidum* genome reveals primary factors for plant terrestrial adaptation. Nat Commun 5:3978–3986

Kasahara H (2016) Current aspects of auxin biosynthesis in plants. Biosci Biotechnol Biochem 80(1):34–42

Korasick DA, Enders TA, Strader LC (2013) Auxin biosynthesis and storage forms. J Exp Bot 64:2541–2555

Lang D, Ullrich KK, Murat F, Fuchs J, Jenkins J, Haas FB, Piednoel M, Gundlach H, Van Bel M, Meyberg R et al (2018) The *Physcomitrella patens* chromosome-scale assembly reveals moss genome structure and evolution. Plant J 93(3):515–533

Leong SS, Chiu W-C, Chou J-C (2009) Gene cloning, nucleotide analysis, and overexpression in *Escherichia coli* of a substrate-specific indole-3-acetyl-L-alanine hydrolase from. *Arthrobacter ilicis*. Bot Stud 50:11–20

Ligrone R, Duckett JG, Renzaglia KS (2012) Major transitions in the evolution of early land plants: a bryological perspective. Ann Bot 109:851–871

Ljung K, Hull AK, Kowalczyk M, Marchant A, Celenza J, Cohen JD, Sandberg G (2002) Biosynthesis, conjugation, catabolism and homeostasis of indole-3-acetic acid in *Arabidopsis thaliana*. Plant Mol Biol 49:249–272

Lu H, Zhao WM, Zheng Y (2005) Analysis of synonymous codon usage bias in Chlamydia. Acta Biochim Biophys Sin (Shanghai) 37(1):1–10

Ludwig-Müller J (2011) Auxin conjugates: their role for plant development and in the evolution of land plants. J Exp Bot 62:1757–1773

Ludwig-Müller J, Decker EL, Reski R (2009a) Dead end for auxin conjugates in *Physcomitrella*? Plant Signal Behav 4:116–118

Ludwig-Müller J, Jülke S, Bierfreund NM, Decker EL, Reski R (2009b) Moss (*Physcomitrella patens*) GH3 proteins act in auxin homeostasis. New Phytol 181(2):323–338

Matasci N, Hung L-H, Yan Z, Carpenter EJ, Wickett NJ, Mirarab S, Nguyen N, Warnow T, Ayyampalayam S, Barker M et al (2014) Data access for the 1,000 plants (1KP) project. GigaScience 3:17

Novak O, Hényková E, Sairanen I, Kowalczyk M, Pospíšil T, Ljung K (2012) Tissue-specific profiling of the *Arabidopsis thaliana* auxin metabolome. Plant J 72(3):523–536

Oksanen J, Blanchet FG, Friendly M, Kindt R, Legendre P, McGlinn P, Minchin D, O'Hara PR, Simpson RB, Solymos GL P (2016) Vegan: community ecology package. R package version 2.4-1

Ortiz-Ramírez C, Hernandez-Coronado M, Thamm A. Catarino B, Wang M, Dolan L, Feijó JAA, Becker JDD (2016) A transcriptome atlas of *Physcomitrella patens* provides insights into the evolution and development of land plants. Mol Plant 9:205–220

Page RD (1996) TREEVIEW: an application to display phylogenetic trees on personal computers. Comput Appl Biosci 12:357–358

Qiu Y-L, Li L, Wang B, Chen Z, Knoop V, Groth-Malonek M, Dombrovska O, Lee J, Kent L, Rest J et al (2006) The deepest divergences in land plants inferred from phylogenomic evidence. Proc Natl Acad Sci USA 103:15511–15516

Qiu Y-L, Li L, Wang B, Chen Z, Dombrovska O, Lee J, Kent L, Li R, Jobson RW, Hendry T, Taylor DW et al (2007) A nonflowering land plant phylogeny inferred from nucleotide sequences of seven chloroplast, mitochondrial, and nuclear genes. Int J Plant Sci 168:691–708

R Core Team (2014) R: a language and environment for statistical computing. R Foundation for Statistical Computing, Vienna

Rensing SA, Lang D, Zimmer AD, Terry A, Salamov A, Shapiro H, Nishiyama T, Perroud PF, Lindquist EA, Kamisugi Y (2008) The *Physcomitrella* genome reveals evolutionary insights into the conquest of land by plants. Science 319(5859):64–69

Rowsell S, Pauptit RA, Tucker AD, Melton RG, Blow DM, Brick P (1997) Crystal structure of carboxypeptidase G2, a bacterial enzyme with applications in cancer therapy. Structure 15:337–347

Saitou N, Nei M (1987) The neighbor-joining method: a new method for reconstructing phylogenetic trees. Mol Biol Evol 4:406–425

Sambrook J, Fritsch EF, Maniatis T (1989) Molecular cloning: a laboratory manual, 2nd edn. Cold Spring Harbor Laboratory Press, Cold Spring Harbor

Sauer M, Robert S, Kleine-Vehn J (2013) Auxin: simply complicated. J Exp Bot 64(9):2565–2577

Shen XX, Hittinger CT, Rokas A (2017) Contentious relationships in phylogenomic studies can be driven by a handful of genes. Nat Ecol Evol 1(5):126

Smolko A, Ludwig-Müller J, Salopek-Sondi B (2018) Auxin amidohydrolases—from structure to function: revisited. Croat Chem Acta 91(2):233–239

Sztein AE, Cohen JD, García de la Fuente I, Cooke TJ (1999) Auxin metabolism in mosses and liverworts. Am J Bot 86:1544–1555

Sztein AE, Cohen JD, Cooke TJ (2000) Evolutionary patterns in the auxin metabolism of green plants. Int J Plant Sci 161:849–859

Thompson JD, Gibson TJ, Plewniak F, Jeanmougin F, Higgins DG (1997) The Clustal X windows interface: flexible strategies for multiple sequence alignment aided by quality analysis tools. Nucleic Acids Res 24:4872–4882

Wellman CH, Osterloff PL, Mohiuddin U (2003) Fragments of the earliest land plants. Nature 425:282–285

Wickham H (2009) ggplot2: elegant graphics for data analysis. Springer, New York

Yu P, Lor P, Ludwig-Müller J, Hegeman AD, Cohen JD (2015) Quantitative evaluation of IAA conjugate pools in *Arabidopsis thaliana*. Planta 241(2):539–548

Yue J, Hu X, Sun H, Yang Y, Huang J (2012) Widespread impact of horizontal gene transfer on plant colonization of land. Nat Commun 3:1152

Zimmer AD, Lang D, Buchta K, Rombauts S, Nishiyama T, Hasebe M, Van de Peer Y, Rensing SA, Reski R (2013) Reannotation and extended community resources for the genome of the non-seed plant *Physcomitrella patens* provide insights into the evolution of plant gene structures and functions. BMC Genom 14:498–511